

Violation of the “information-disturbance relationship” in a multipartite system

A. Thilagam

*Information Technology, Engineering and the Environment,
Mawson Institute, University of South Australia, Australia 5095*

(Dated: November 8, 2018)

The effect of measurement attributes such as the quantum level of precision and finite duration on the classical and quantum correlations is analysed for a pair of qubits immersed in a common reservoir. We show that the quantum discord is enhanced as the precision of the measuring instrument is increased, and both the classical correlation and the quantum discord undergo noticeable changes during finite-time measurements performed on a neighboring partition. The implication of these results on the “information-disturbance relationship” is examined, with critical analysis of the delicate roles played by quantum non-locality and non-Markovian dynamics in the violation of this relationship, which appears surprisingly for a range of measurement attributes. This work highlights that the fundamental limits of quantum mechanical measurements can be influenced by non-classical correlations such as the quantum discord.

PACS numbers: 03.67.-a, 03.65.Ta, 03.65.Yz

I. INTRODUCTION

The role of measurements in quantum correlation and decoherence processes presents one of the most challenging areas of investigation of quantum systems [1–9]. Some progress has been made in the understanding of the links between quantum measurements and decoherence processes which results in the breakdown of phases in the superposed states [10]. In the “decoherence scheme”, a quantum system which survives while in contact with an environment is guided to its pointer states [11]. The view that an open quantum system is equivalent to a system which is continuously measured by its environment has been examined using various approaches [12, 13]. However, questions still exist with regard to the links between quantum correlations and non-locality, mainly due to difficulties in formulating a rigorous definition for the latter due to ongoing debates on the non-objectivity-non-locality issue. Quantum measurements have been associated with the collapse of the wavefunction of the observed system, unlike other kinds of interactions. The details of the detection of the exact point at which a classical world emerges from a group of interacting quantum systems, and the various factors which trigger such transitions remains unclear. Recent works [14, 15] have shown that invasive measurements which have an influence on the dynamics of the monitored system can give rise to classicality in quantum systems.

Quantum measurements have also taken more important roles in recent years due to their incorporation in the definition of several measures of quantum correlations, including the quantum discord [16–18]. This entity has been known to possess more generalized properties than other well established measures such as the Wootters concurrence [19], and is useful in differentiating processes which are essentially quantum from those that incorporate generically non-classical features [20–24]. The quantum discord of a specific system is obtained by performing a set of positive-operator-valued measurements (POVM) in a neighboring partition. At zero quantum discord, a measurement procedure allows external observers to obtain all information about a bipartite system without disturbing it. Two quantum systems can be considered as purely classically linked if the measurements performed on one system does not affect the adjacent system.

Recently, the tradeoff between information gained due to quantum measurement and the disturbance on the observed quantity, has been examined in several works [25–29]. One study [26] showed that an informative measurement affects at least one state of the system, and the quantity of disturbance on the state is limited by the amount of information that can distinguish the input and corresponding output states. This trade-off between the magnitude of information obtained via quantum measurements and disturbance on the evolution of the system could be reinterpreted using the Heisenberg uncertainty principle [27–29]. Heisenberg [30] first raised the idea that any attempt to measure the position of a particle with higher precision will result in a greater disturbance as quantified by the mean square deviations of the momentum measurements. In a recent experimental study [31] involving weak measurements, Heisenberg’s “measurement-disturbance relationship” was seen to be violated.

The current study is aimed at examining the attributes of the measurement process and imperfections which distort the quantum correlations present in entangled systems. This provides an natural extension to the problem of whether an entropic information-measurement attributes relations exist as well. We focus on two key attributes: a) the measurement duration, and, b) the quantum level precision for a model system of a qubit pair immersed in a common reservoir. In order to keep the numerical analysis tractable, we adopt the Feynman’s path integral framework [32, 33] to interpret quantum measurements, and in particular, employ a variant of this formalism based on the restricted

path integral formalism [9, 34]. Within the restricted path framework, the continuous measurement of a quantity with a given result is monitored by constraints imposed on the Feynman's path integral. Accordingly an anti-Hermitian term is added to the Hamiltonian describing the dynamics of the measured system. In the presence of non-Hermitian terms which appear in highly precise measurements, the measured system may evolve via one or more complex routes, and the final readout is ill-defined. The key feature in this work is the possibility that projections associated with imperfect measurements can be performed, a departure from conventional treatments. The restricted path integral is appealing as it is dependent solely on the information gained from the measurement procedure, and independent of the detailed construct of the measuring device. The dependence on generic features of the secondary system acting as the observer or measuring device is therefore reduced. This provides some simplification when investigating the effects of measurements.

This paper is organized as follows. In Section II we describe the restricted path integral approach for energy measurements incorporating the non-ideal attributes of the measuring device. The influence of non-ideal measurements on a qubit is detailed in Section II A. Description of the quantum discord measures and details of the qubit pair system under study is provided in Section III, including an analysis of the influence of critical parameters in the violation of a Bell inequality associated with the quantum state of the qubit pair. In Section IV, the effect of the measurement precision and finite time duration on the quantum correlation measure is evaluated and numerical results are presented. The information-measurement precision trade-off relations is examined in Section V and the implication of results obtained in Section IV on the “information-disturbance relationship” is discussed. In Section VI non-Markovianity as quantified by the fidelity difference is used to analyze the flow of information during quantum measurements, and the issues of quantum non-locality and non-Markovian dynamics during violation of the “information-disturbance relationship”, is examined. The conclusion is provided in Section VII.

II. THE RESTRICTED PATH INTEGRAL PATH APPROACH FOR ENERGY MEASUREMENTS

We recall the two key elements in Feynman's path integral formalism [32, 33]: the first involves the superposition principle which yields the transition amplitude for a given quantum process, and in the absence of measurements. Under this scheme, the probability amplitude of the transition from the initial to the final state of the system is obtained via summation of the amplitudes of all possible paths which could also interfere with each other. The second feature in Feynman's formalism involves the weight attached to the individual paths which are involved during summation, this weight provides a measure of contribution of each constituent path.

The restricted path integral is derived [9, 34–36] from the Feynman path integral via the introduction of a weight functional within the integrand of the various paths involved in the summation process. We recall that the Feynman's propagator, $K_{[E]}(q', \tau; q, 0)$ in the phase-space representation at time τ is given by [32, 33]

$$K(q', \tau; q, 0) = \int d[q]d[p] e^{\frac{i}{\hbar} \int_0^\tau [p\dot{q} - \hat{H}_0(q,p)] dt} \quad (1)$$

where \hat{H}_0 is the Hamiltonian of the closed (unmeasured) quantum system and $[p]$ and $[q]$ are the paths in the momentum and configuration spaces respectively. In Mensky's formalism, the output of a quantum system subjected to measurement is expressed in terms of constrained paths linked to the measured system via a weight functional $w_{[E]}$ [9]. The functional may assume a Gaussian form with a damping magnitude that is proportional to the squared difference between the observed value along the paths and the actual measurement result. Thus a system subjected to measurement evolves via a propagator which modifies Eq.(1) according to [36, 37]

$$K_{[E]}(q', \tau; q, 0) = \int d[q]d[p] e^{\frac{i}{\hbar} \int_0^\tau [p\dot{q} - \hat{H}_0(q,p)] dt} w_{[E]} \quad (2)$$

. This relation highlights the dependence of a selected measurement output such as E for a measuring instrument that incurs an error E_r during a measurement duration, τ

The sensitivity or error during measurements of the energy levels of a two-level system is known to influence inter-level transitions [37–39]. In a recent work [40], singularities known as exceptional points [41] are shown to appear at the branch point of eigenfunctions at a critical measurement precision E_r^c . The significance of the results from Mensky's formalism lies in the inclusion of attributes of the measuring device, which determines the dynamics of the quantum system under observation. This has obvious implications for the evaluation of the quantum discord in quantum systems, as will be shown later in this work. The use of the Gaussian measure, $w_{[E]} = \exp \left\{ -\frac{\langle (H_0 - E)^2 \rangle}{\Delta E^2} \right\}$ enables the effect of the measurement to be incorporated via the effective Hamiltonian [37, 38] for a two-level system

$$\hat{H}_{eff} = \hat{H}_0 - i \frac{\hbar}{\tau E_r^2} (\hat{H}_0 - E)^2 \quad (3)$$

where $\langle \dots \rangle$ denotes the time-average for the duration τ during which measurement was performed. As noted earlier, E (see Eq.(2)) is the selected measurement output after a time τ and E_r is the error made during the measurement of the energy, E . It is evident that maximization of the product τE_r ensures minimal disturbance associated with the measurement process. This product term is linked to the uncertainty principle, so that a lower limit τE_r would ensure maximal disturbance on the monitored system. A large error E_r and duration τ are key attributes of a weak measurement, and the finite duration τ yields a degree of uncertainty in energy of the observed quantum system. We therefore consider a non-Hermitian term small enough so that the system under observation evolves as $i\hbar \frac{\partial}{\partial t} |\psi(t)\rangle = H_{eff} |\psi(t)\rangle$. By expanding the state of the system within the unperturbed basis states $|n\rangle$ of the unmeasured system with Hamiltonian \hat{H}_0 as $|\psi(t)\rangle = \sum_n C_n(t) |n\rangle$, the coefficients $C_n(t)$ can be determined using the Schrödinger equation based on the Hamiltonian in Eq.(3).

A. Influence of non-ideal measurements on a qubit

We consider the Hamiltonian \hat{H}_0 of the unmeasured qubit with energies E_1 (E_2) at state $|0\rangle$ ($|1\rangle$) of the form

$$\hat{H}_0 = -\hbar \left(\frac{\Delta\omega}{2} \sigma_z + V(t) \sigma_x \right), \quad (4)$$

where the Pauli matrices $\sigma_x = |0\rangle\langle 1| + |1\rangle\langle 0|$, $\sigma_z = |1\rangle\langle 1| - |0\rangle\langle 0|$, $\Delta\omega = 2(E_1 + E_2)$ and the potential $V(t)$ which induces transitions between the two levels. The perturbation potential terms are taken to be $V_{00} = V_{11} = 0$ and $V_{01} = V_{10}^* = V_0 e^{i\omega(t-t_0)}$ with V_0 as a real number. The state of the measured system, $|\psi(t)\rangle$ evolves as [40]

$$|\psi(t)\rangle = e^{-i(E_1 - i\lambda_1/4)t} C_1(t) |0\rangle + e^{-i(E_2 - i\lambda_2/4)t} C_2(t) |1\rangle \quad (5)$$

where $\lambda_1 = \frac{(E_1 - E)^2}{2\tau E_r^2}$ and $\lambda_2 = \frac{(E_2 - E)^2}{2\tau E_r^2}$ for a renormalized E_r .

The coefficients $C_1(t)$, $C_2(t)$ in Eq.(5) are obtained using

$$\begin{bmatrix} C_1(t) \\ C_2(t) \end{bmatrix} = \begin{bmatrix} \cos \kappa t - i\alpha_1 & -i\alpha_2 \\ -i\alpha_2 & \cos \kappa t + i\alpha_1 \end{bmatrix} \begin{bmatrix} C_1(0) \\ C_2(0) \end{bmatrix}, \quad (6)$$

where $\alpha_1 = \cos \theta \sin \kappa t$, $\alpha_2 = \sin \theta \sin \kappa t$, $\cos \theta = \frac{q}{\kappa}$, $\kappa = \sqrt{q^2 + V_0^2}$, $q = \frac{1}{2}(\omega - \Delta E + i\Omega/2)$, $\Delta E = (E_2 - E_1)$, and $\Omega = \lambda_2 - \lambda_1$. The qubit states of the monitored system therefore incorporate non-Hermitian terms which are functions of the measurement attributes

$$\begin{aligned} |\chi_s(t)\rangle &= e^{-\lambda_t t/4} (\cos \kappa t - i \cos \theta \sin \kappa t) |0\rangle \\ &\quad - i e^{-\lambda_t t/4} \sin \theta \sin \kappa t |1\rangle \\ |\chi_a(t)\rangle &= e^{-\lambda_t t/4} (\cos \kappa t + i \cos \theta \sin \kappa t) |1\rangle \\ &\quad - i e^{-\lambda_t t/4} \sin \theta \sin \kappa t |0\rangle, \end{aligned} \quad (7)$$

where $\lambda_t = \frac{\Delta E^2}{2\tau E_r^2}$. For measurement procedures which introduce very large errors, $E_r \rightarrow \infty$, $\lambda_1 = \lambda_2 = \lambda_t = \cos \theta = 0$, and the qubit oscillates coherently between the two levels with the Rabi frequency $2\kappa = 2V_0$ as is well known in the unmeasured system.

For a system in which the initial state at $t = 0$ is $|1\rangle$ and the final state at time t is either $|1\rangle$ or $|0\rangle$, the probability P_{11} (P_{10}) of the system to be in the state $|1\rangle$ ($|0\rangle$) depends on the relation between V_0 and λ_t . At the resonance frequencies, $\omega = \Delta E$, the Rabi frequency $2\kappa_0 = (4V_0^2 - (\frac{\lambda_t}{2})^2)^{1/2}$, and $\cos \theta = -i\lambda_t/4\kappa_0$. There exists two tunneling regimes with $V_0 > \frac{\lambda_t}{4}$ ($V_0 < \frac{\lambda_t}{4}$) applicable to the coherent (incoherent) cases. For the coherent tunneling regime we have

$$P_{11} = e^{-\lambda_t t/2} \left[\cos \kappa_0 t - \frac{\lambda_t}{4\kappa_0} \sin \kappa_0 t \right]^2 \quad (8)$$

$$P_{10} = e^{-\lambda_t t/2} \frac{V_0^2}{\kappa_0^2} \sin^2 \kappa_0 t, \quad (9)$$

where $\lambda_t = \frac{(E_2 - E_1)^2}{2\tau E_r^2}$. The total probabilities, $P_{11} + P_{10} \leq 1$, the loss of normalization is dependent on the measurement precision, E_r as expected. For the system undergoing incoherent tunneling, we replace $\sin[x]$ ($\cos[x]$) by $\sinh[x]$ ($\cosh[x]$). The dynamics at the exceptional point occurs at $\kappa_0 = 0$, $V_0 = \frac{\lambda_t}{4}$, and both regimes merge to a point in topological space. The two-level system can be seen as a non-ideal dissipative quantum system due to its coupling to a multitude of decay states associated with the measurement process.

III. CLASSICAL CORRELATION AND QUANTUM DISCORD

Following the formulation of quantum discord in Refs.[16–18], we express the quantum mutual information of a composite state ρ of two subsystems A and B as $\mathcal{I}(\rho) = S(\rho_A) + S(\rho_B) - S(\rho)$ for a density operator in $\mathcal{H}_A \otimes \mathcal{H}_B$. ρ_A (ρ_B) is the reduced density matrix associated with A (B) and $S(\rho_i)$ ($i=A,B$) denotes the well known von Neumann entropy of the density operator ρ_i , where $S(\rho) = -\text{tr}(\rho \log \rho)$. The mutual information can also be written in terms of quantum conditional entropy $S(\rho|\rho_A) = S(\rho) - S(\rho_A)$ as

$$\mathcal{I}(\rho) = S(\rho_B) - S(\rho|\rho_A) \quad (10)$$

A series of one-dimensional orthogonal projectors $\{\Pi_k\}$ induced in \mathcal{H}_A leads to different outcomes of the measurement in \mathcal{H}_B via the post measurement conditional state

$$\rho_{B|k} = \frac{1}{p_k} (\Pi_k \otimes \mathbb{I}_B) \rho (\Pi_k \otimes \mathbb{I}_B) \quad (11)$$

where the probability $p_k = \text{tr}[\rho(\Pi_k \otimes \mathbb{I}_B)]$ and $\{\Pi_k\}$ denote the one-dimensional projector indexed by the outcome k . From the cumulative effect of the mutually exclusive measurements on A , we obtain a conditional entropy of the subsystem B based on $\rho_{B|k}$

$$S(\rho|\{\Pi_k\}) = \sum_k p_k S(\rho_{B|k}) \quad (12)$$

which is used to obtain the measurement induced mutual information $\mathcal{I}(\rho|\{\Pi_k\}) = S(\rho_B) - S(\rho|\{\Pi_k\})$. The classical correlation measure based on optimal measurements made on A is obtained as [16–18]

$$\mathcal{C}_A(\rho) = \sup_{\{\Pi_k\}} \mathcal{I}(\rho|\{\Pi_k\}) \quad (13)$$

The difference in $\mathcal{I}(\rho)$ and $\mathcal{C}_A(\rho)$ yields the non symmetric quantum discord $\mathcal{D}_A(\rho) = \mathcal{I}(\rho) - \mathcal{C}_A(\rho)$. The discord $\mathcal{D}_B(\rho)$ associated with measurements on subsystem B can be evaluated likewise, and in general $\mathcal{D}_A(\rho) \neq \mathcal{D}_B(\rho)$. Measurements made on a neighboring partition is the key to determining the classical correlation measure between the subsystems.

A. A qubit pair immersed in a common reservoir

The joint evolution of a pair of two-level qubit subsystems, A, B undergoing decoherence in a common reservoir is determined by a completely positive trace preserving map expressed in the operator-sum form [42–44]

$$\varepsilon(\rho_{AB}) = \sum_{i,j} \Gamma_i(A) \Gamma_j(B) \rho_{AB} \Gamma_i^\dagger(B) \Gamma_j^\dagger(A), \quad (14)$$

where $\Gamma_i(A)$ ($\Gamma_i(B)$) is the Kraus operator associated with the decoherence process at A (B). For the phase flip channel in which there is loss of quantum information with conservation of energy, the Kraus operators are given in the basis $\{|0\rangle, |1\rangle\}$ for both subsystems, $k = A, B$ as [21, 42] $\Gamma_0(A) = \text{diag}(\sqrt{1-p/2}, \sqrt{1-p/2}) \otimes \mathbf{1}_B$, $\Gamma_1(A) = \text{diag}(\sqrt{p/2}, -\sqrt{p/2}) \otimes \mathbf{1}_B$, $\Gamma_0(B) = \mathbf{1}_A \otimes \text{diag}(\sqrt{1-p/2}, \sqrt{1-p/2})$ and $\Gamma_1(B) = \mathbf{1}_A \otimes \text{diag}(\sqrt{p/2}, -\sqrt{p/2})$. The parameter $p = 1 - \exp(-\gamma t)$, where γ denotes the phase damping rate.

To simplify the numerical analysis, we consider a joint state of the pair of two-level qubit subsystems, A, B in an initial X -type state with maximally mixed marginals ($\rho_{A(B)} = I_{A(B)}/2$, $S(\rho_A(t)) = S(\rho_B(t)) = 1$). The density matrix appears in the form $\rho(0) = \frac{1}{4}[I + \sum_{i=1,2,3} c_i \sigma_A^i \otimes \sigma_B^i]$, where I is the identity operator associated with the qubit pair, σ_A^i , and σ_B^i , and σ_j^i ($j = A, B$, $i = 1, 2, 3$) are the Pauli operators of each qubit. c_i ($0 \leq |c_i| \leq 1$) are real numbers, with the Werner states sharing a common $|c_1| = |c_2| = |c_3| = c$ and $c=1$ for the Bell basis states. We assume that the usual unit trace and positivity conditions of the density operator ρ are satisfied. For the class of states where $|c_1| = |c_2| = c$, $|c_3| = c_3$, the evolution of the joint system is described by the matrix

$$\rho_{A,B}(t) = \frac{1}{4} \begin{pmatrix} 1+c_3 & 0 & 0 & 0 \\ 0 & 1-c_3 & 2ce^{\mu^*t} & 0 \\ 0 & 2ce^{\mu t} & 1-c_3 & 0 \\ 0 & 0 & 0 & 1+c_3 \end{pmatrix}, \quad (15)$$

where $\mu = [-2\gamma - i(\Delta\omega_A - \Delta\omega_B)]t$, and as noted earlier γ is the phase damping rate. To simplify the analysis, we have considered the same damping rate for the two qubit subsystems. $\Delta\omega_i, i = A, B$ denotes the difference in energy levels of each qubit subsystem, we consider equivalent energy levels in the qubit pair. The mutual information of state $\rho_{A,B}$ in Eq. (15) is evaluated using $\mathcal{I}(\rho_A : \rho_B) = 2 + \sum_{i=1}^4 \lambda_i \log \lambda_i$ where the eigenvalues λ_i of $\rho_{A,B}$ are $\lambda_{1,2} = \frac{1}{4}(1 + c_3)$, $\lambda_3 = \frac{1}{4}(1 - c_3 + 2ce^{-2\gamma t})$ and $\lambda_4 = \frac{1}{4}(1 - c_3 - 2ce^{-2\gamma t})$

B. Influence of c_3 and c in the violation of a Bell inequality

The violation of the CHSH-Bell inequality function \mathcal{B} quantifies quantum nonlocal correlations which cannot be created by classical means [45, 46]. The CHSH inequality Bell function \mathcal{B} is $|\mathcal{B}| \leq 2$, where $\mathcal{B} = M(\vec{a}, \vec{b}) - M(\vec{a}, \vec{b}') + M(\vec{a}', \vec{b}) + M(\vec{a}', \vec{b}')$, where $M(\vec{a}, \vec{b})$ is the correlated results (± 1) arising from the measurement of two qubits in directions \vec{a} and \vec{b} . The CHSH-Bell inequality is violated when \mathcal{B} exceeds 2, and the correlations is considered inaccessible by any classical means of information transfer, while for values less than 2, the local hidden-variable theory is seen to satisfy the CHSH-Bell inequality.

We first investigate the influence of parameters $c_1 = c_2 = c$ and c_3 in a possible violation of the CHSH-Bell inequality. These results will be compared with the effect of c and c_3 on classical and quantum correlations in the next Section. For the density matrix in Eq. (15), \mathcal{B} based on correlations averages, is obtained using the following relations [47]

$$\begin{aligned} \mathcal{B}(t, c, c_3) &= \text{Max} \{ \mathcal{B}_1(t, c, c_3), \mathcal{B}_2(t, c, c_3) \} \\ \mathcal{B}_1(t, c, c_3) &= 2\sqrt{e^{-4gt}c^2 + c_3^2} \\ \mathcal{B}_2(t, c, c_3) &= 2\sqrt{2}ce^{-2gt} \end{aligned} \quad (16)$$

In general, the interplay of several parameters (c, c_3, t, g) makes it a complex problem to examine the non-locality of the two-qubit density matrix, $\rho_{A,B}$. To simplify the approach, we note that the eigenvalues λ_i of $\rho_{A,B}$ in Eq. (15) need to satisfy the positivity criteria of non-negative values. To this end, $\lambda_4 = \frac{1}{4}(1 - c_3 - 2ce^{-2\gamma t})$ is most susceptible to violating this criteria when $c_3^m = 1 - 2ce^{-2\gamma t}$. Figure 1a,b show values of $\mathcal{B}(t, c, c_3)$ as a function of c, t , at two damping rates g , with $c_3 = c_3^m$. The results show that with increasing c , the system is likely to violate the Bell inequality during the initial period of measurement. There are subtle differences in the system non-locality arising from use of low and high g as can be inferred from Eq. (16). In Figure 1c where c_3 is not constrained, the system best exhibits classical features at low $c \approx 0.1$ and $c_3 \sim c$. There is a gradual shift towards possible violation of the CHSH-Bell inequality as c is increased, when λ_4 becomes negative.

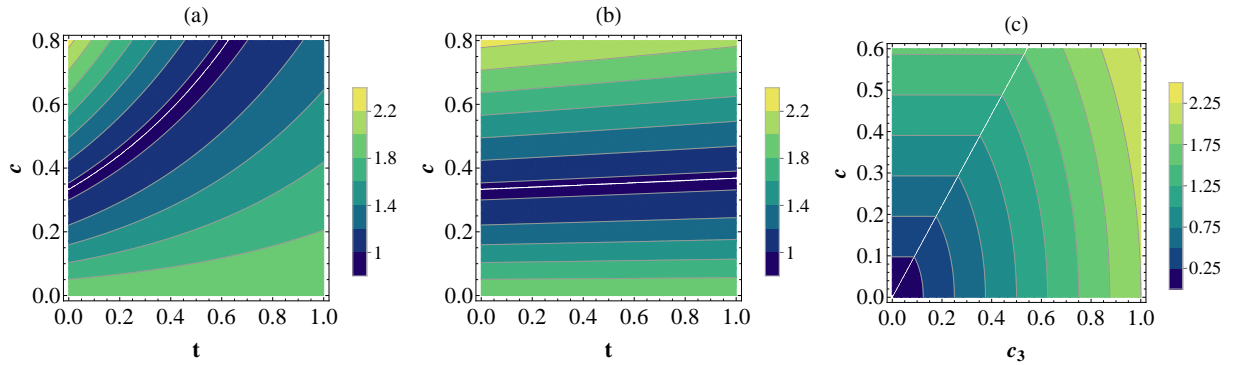


FIG. 1: (a) Bell inequality, \mathcal{B} (Eq. (16)) as function of unitless t/τ ($0 < t < \tau$) and c . c_3 is fixed at $c_3 = 1 - 2ce^{-2\gamma t}$. The measurement time duration, $\tau = 2\pi/V_0=1$, $c = 0.15$, and phase damping rate $g = \gamma\tau=0.7$. (b) All same except $g = \gamma\tau=0.05$. (c) Bell inequality, \mathcal{B} (Eq. (16)) as function of c and c_3 , $t=\tau$.

IV. MEASUREMENT PRECISION AND QUANTUM CORRELATIONS

The classical correlation measure is obtained through all possible local measurements on one of the subsystems, say A . For the ideal case of a local measurement that is instantaneous, we utilize a set of orthogonal projectors

$\{\Pi_k = |\theta_k\rangle\langle\theta_k|, k = \parallel, \perp\}$, which are defined in terms of the orthogonal states

$$\begin{aligned} |\theta_{\parallel}\rangle &= \cos\theta |0\rangle + e^{i\phi} \sin\theta |1\rangle, \\ |\theta_{\perp}\rangle &= e^{-i\phi} \sin\theta |0\rangle - \cos\theta |1\rangle, \end{aligned} \quad (17)$$

where $0 \leq \theta \leq \pi/2$ and $0 \leq \phi \leq 2\pi$. In a recent work, Galve et. al. [48] showed that orthogonal measurements are sufficient to evaluate the quantum discord pertaining to rank 2 states of two qubit systems, but provide tight upper bounds for higher rank (3 and 4) states.

Using Eq. (7) as a basis, we modify the projection operators in Eq. (17) using generalized projectors that incorporate measurement attributes

$$\begin{aligned} |\theta_{\parallel}\rangle_p &= R(\theta) |0\rangle + e^{i\phi} S(\theta) |1\rangle, \\ |\theta_{\perp}\rangle_p &= e^{-i\phi} S(\theta) |0\rangle - R(\theta) |1\rangle, \end{aligned} \quad (18)$$

The terms $R(\theta) = e^{-\lambda_r t/4} (\cos\theta - i \frac{\lambda_r t}{4\theta} \sin\theta)$ and $S(\theta) = e^{-\lambda_r t/4} \frac{\sqrt{\theta^2 + (\lambda_r t/4)^2}}{\theta} \sin\theta$ with $\lambda_r = \frac{\Delta E^2}{2\tau E_r^2}$, ΔE being the energy difference between the $|1\rangle$ and $|0\rangle$ states of the qubit. In the limit of $\lambda_r \rightarrow 0$, Eq. (18) reverts back to the orthogonal set in Eq. (17). It is implicit that the orthogonal measurement projections in Eq. (18) may be in a state of evolution during the measurement process.

The generalized measurements as specified by the constituent maps in Eq. (18) can be projected as follows

$$\begin{aligned} &\frac{1}{2} |\theta_{\parallel}\rangle_p \langle\theta_{\parallel}|_p + \frac{1}{2} |\theta_{\perp}\rangle_p \langle\theta_{\perp}|_p, \\ &= \begin{pmatrix} |R(\theta)|^2 + |S(\theta)|^2 & 0 \\ 0 & |R(\theta)|^2 + |S(\theta)|^2 \end{pmatrix}, \\ &= \begin{pmatrix} 1 & 0 \\ 0 & 1 \end{pmatrix}, \quad t = \lambda_r = 0 \end{aligned} \quad (19)$$

The incorporation of measurement attributes (τ, p) therefore leads to non-preservation of the trace of the density matrix in Eq. (19). This can be attributed to loss of the particle from the system due to the observational mapping process. The dependence of the projected states given in Eq. (18) on the measurement attributes, τ and λ_r also results in the dependence of the classical correlation on these same attributes, and we examine such a relationship next.

The reduced density matrices, $\rho_B^{(k)}$ of the neighboring subsystem B in accordance with the two projective measurements ($p_{\parallel} = p_{\perp} = 1/2$) in subsystem A are obtained as

$$\rho_B^{\parallel} = \begin{pmatrix} \frac{1}{2}(1 - c_3 e^{-pt/2} [\varphi_1 - \varphi_2]) & \frac{1}{2} c e^{-2gt} \varphi_1 \varphi_2 \\ \frac{1}{2} c e^{-2gt} \varphi_1 \varphi_2 & \frac{1}{2}(1 + c_3 e^{-pt/2} [\varphi_1 - \varphi_2]) \end{pmatrix}, \quad (20)$$

$$\rho_B^{\perp} = \begin{pmatrix} \frac{1}{2}(1 + c_3 e^{-pt/2} [\varphi_1 - \varphi_2]) & -\frac{1}{2} c e^{-2gt} \varphi_1 \varphi_2 \\ -\frac{1}{2} c e^{-2gt} \varphi_1 \varphi_2 & \frac{1}{2}(1 - c_3 e^{-pt/2} [\varphi_1 - \varphi_2]) \end{pmatrix}. \quad (21)$$

where $\varphi_1 = \cos^2\theta - (\frac{pt}{4\theta})^2 \sin^2\theta - \frac{\xi^2}{\theta^2} \sin^2\theta$, $\varphi_2 = \frac{\xi^2}{\theta^2} \sin^2\theta$ and $\xi = \sqrt{\theta^2 + (pt/4)^2}$. $g = \gamma\tau$, the unitless time, t is obtained via division with the measurement duration, $\tau = 2\pi/V_0$ and the dimensionless precision parameter, $p = \lambda_r\tau$. The eigenvalues of the two reduced density matrices, $\rho_B^{(k)}$ of the neighboring subsystem B are obtained as

$$\begin{aligned} \zeta_{1,2}^{(k)} &= \frac{1}{2}(1 \pm \Theta), \\ \Theta^2 &= c_3^2 e^{-pt} [\varphi_1 - \varphi_2]^2 + 4c^2 e^{-4gt} e^{-pt} \varphi_1 \varphi_2 \end{aligned} \quad (22)$$

Using Eq. (22), we obtain $S(\rho_B^{\parallel}) = S(\rho_B^{\perp}) = -\text{tr}(\rho \log \rho) = R(\Theta) = -\frac{1-\Theta}{2} \log_2 \left[\frac{1-\Theta}{2} \right] - \frac{1+\Theta}{2} \log_2 \left[\frac{1+\Theta}{2} \right]$. The classical correlation given in Eq. (13) is evaluated using

$$\mathcal{C}(\rho) = 1 - \min_{\theta, \phi} R(\Theta), \quad (23)$$

Further evaluation of $\mathcal{C}(\rho)$ is simplified by the elimination of the parameter ϕ due to the choice of similar parameters, $|c_1| = |c_2| = c$. The maximal value of Θ is not only dependent on c_3, c, γ , but also on the precision parameter p and the measurement duration τ . It is obvious from Eq. (22), that the influence of the phase damping rate becomes pronounced at $c > c_3$.

The quantum discord is evaluated using

$$\mathcal{D}(\rho) = 2 + \sum_{k=1}^4 \lambda_k \log_2 \lambda_k - \mathcal{C}(\rho), \quad (24)$$

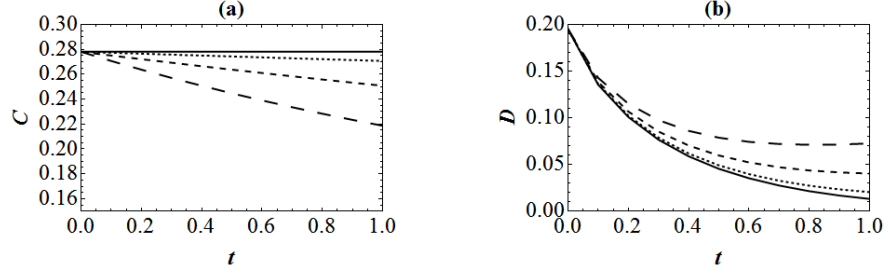


FIG. 2: (a) Classical correlation \mathcal{C} as function of t ($0 < t < \tau$) for various values of the measurement precision p . τ the measurement time duration is set at 1 and $g = \gamma\tau = 0.6$, where γ is the phase damping rate. The real numbers $c_1 = c_2 = c = 0.2$ and $c_3 = 0.6$. The curves from top to bottom correspond to the unitless measurement precision, $p = 0, 0.05, 0.2, 0.5$. and (b) Quantum discord \mathcal{D} as function of t ($0 < t < \tau$) for various values of the measurement precision $p = 0.5, 0.2, 0.05, 0$ (top to bottom). All other parameters are the same as in (a).

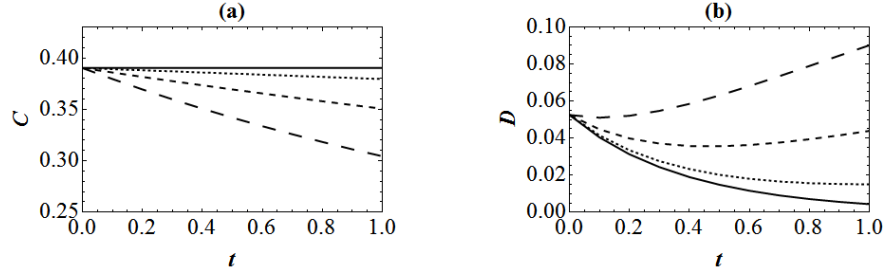


FIG. 3: a) Classical correlation \mathcal{C} as function of t ($0 < t < \tau$) for various values of the measurement precision p . τ the measurement time duration is set at 1 and $g = \gamma\tau = 0.6$. The real numbers $c_1 = c_2 = c = 0.1$ and $c_3 = 0.7$. The curves from top to bottom correspond to the unitless measurement precision, $p = 0, 0.05, 0.2, 0.5$. and (b) Quantum discord \mathcal{D} as function of t for various values of the measurement precision $p = 0.5, 0.2, 0.05, 0$ (top to bottom). All other parameters are the same as in (a).

Figures 2, 3 highlight changes in the classical correlation \mathcal{C} and quantum discord \mathcal{D} as function of t ($0 < t < \tau$), based on numerical evaluation of Eqs. (22), (23), (24) and the eigenvalues λ_i of $\rho_{A,B}$ in Eq. (15). \mathcal{C} and \mathcal{D} undergo noticeable changes due to finite-time measurements on a neighboring partition at non-zero p , for input parameters $c_3 > c$. Figures 2b and 3b show that the quantum discord \mathcal{D} is enhanced, with a corresponding decrease in \mathcal{C} as p is increased. The enhancement in the quantum discord \mathcal{D} is pronounced at a higher ratio $\frac{c_3}{c}$. However at $c > c_3$, the numerically evaluated classical correlation was noted to be almost insignificant, $\mathcal{C} \approx 0.01$ and \mathcal{D} was seen to be independent of p . These results indicate a trend towards more non-classical behaviour at increased p for the case when $c_3 > c$, however it is not immediately clear why a low \mathcal{C} was obtained at $c_3 < c$. Figures 4 and 5 illustrate the changes in \mathcal{C} and \mathcal{D} due to the dephasing rate g for various values of the measurement precision p . At $c < c_3$, the classical correlation \mathcal{C} remains independent of g , a trend that appears only beyond a critical g at $c > c_3$. This has also been noted in earlier works [21, 22] for the specific case, $p=0$.

Imperfect measurements carried out on the subsystem A therefore enhance the non-classical correlations of the adjacent subsystem B at $c_3 > c$, while there is less impact of such measurements for $c < c_3$. A possible explanation may be obtained from results of the CHSH-Bell inequality, \mathcal{B} in Figure 1. It appears that states which exhibit greater classical features (at low c , $c_3 > c$), are more likely to have reduced \mathcal{C} and increased \mathcal{D} with measurements carried out in an adjacent subsystem. On the other hand, states which are close to CHSH-Bell inequality violation ($c > c_3$) are close to obeying non-locality and less influenced by any imprecise measurement procedures.

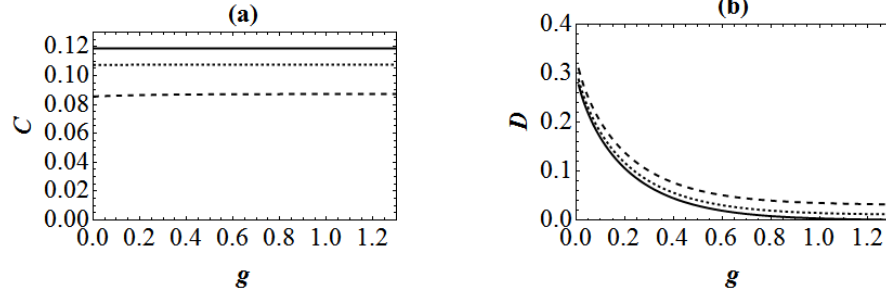


FIG. 4: (a) Classical correlation \mathcal{C} as function of the unitless $g = \gamma\tau$ where γ is the phase damping rate, for various values of the measurement precision p at $t=1$. The real numbers $c_1=c_2=c=0.3$ and $c_3=0.4$. The curves from top to bottom correspond to the unitless measurement precision, $p=0, 0.2, 0.7$. and (b) Quantum discord \mathcal{D} as function of g at $t=1$. for various values of the measurement precision $p=0.7, 0.2, 0$ (top to bottom). All other parameters are the same as in (a).

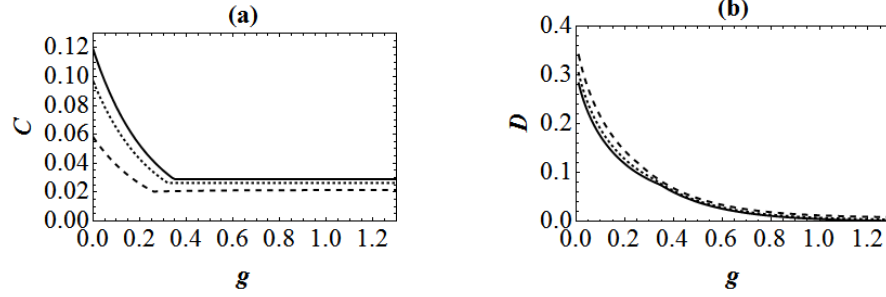


FIG. 5: (a) Classical correlation \mathcal{C} as function of the unitless $g = \gamma\tau$ where γ is the phase damping rate, for various values of the measurement precision p at $t=1$. The real numbers $c_1=c_2=c=0.4$ and $c_3=0.2$. The curves from top to bottom correspond to the unitless measurement precision, $p=0, 0.2, 0.7$. and (b) Quantum discord \mathcal{D} as function of g at $t=1$ at measurement precision $p=0.7, 0.2, 0$ (top to bottom). All other parameters are the same as in (a).

V. INFORMATION-MEASUREMENT PRECISION TRADE-OFF

The results in Section IV highlight the effect of disturbance on the classical and non-classical correlations of the adjacent reduced density matrix, $\rho_B^{(k)}$. This disturbance is quantified by the measurement precision p and finite time duration τ associated with the imperfect projective measurements (Eq. (18)) on subsystem A . In this Section, we examine the implications of these results on the “information-disturbance relationship” on subsystem B as a result of imperfect measurements on subsystem A . We note the two sources of uncertainty (p, τ) which give rise to a probabilistic distribution of the quantity being measured.

Two important measures will be used to examine the tradeoff between information gained due to quantum measurement and the disturbance caused during observation: fidelity and trace distance. The fidelity, \mathcal{F} [49] which quantifies the distance between two states appear as

$$F[\rho_1, \rho_2] = \left\{ \text{Tr} \left[\sqrt{\sqrt{\rho_1} \rho_2 \sqrt{\rho_1}} \right] \right\}^2, \quad (25)$$

and is bounded by $0 \leq F[\rho_1, \rho_2] \leq 1$. The measurement disturbance on the dynamics of a system can be quantified using [26]

$$D_i = 1 - F[\rho_1, \rho_2] \quad (26)$$

Based on the reduced density matrices $\rho_B^\parallel(t=0, p=0)$ and $\rho_B^\parallel(t, p)$ (Eq. (20)), the disturbance, D_i can be evaluated as a function of t and p .

To quantify the information gained from the system, we define the uncertainty $H(\nu)$ based on the parameter ν where

$$\nu = \frac{1}{2} - \frac{1}{2} T_d(\rho_1, \rho_2) \quad (27)$$

The trace distance, T_d between density matrices, ρ_1, ρ_2 , is given by half of the trace norm of the difference of the matrices as $T_d(\rho_1, \rho_2) = \frac{1}{2}\text{Tr}[\rho_1 - \rho_2]$ and $H(x) = -x \log_2 x - (1-x) \log_2 (1-x)$. In order to analyse the influence of the precision p and t , we consider $\rho_1 = \rho_B^\parallel(t=0, p=0)$ and $\rho_2 = \rho_B^\parallel(t, p)$. It remains to investigate the information-disturbance tradeoff relation [26]

$$1 - F[\rho_1, \rho_2] \geq 1 - H(\nu(p, t)) \quad (28)$$

where the mutual information ($1-H(\nu(p, t))$) is evaluated using ν (Eq. (27)) for given values of the measurement attributes, p, t . Eq. (28) specifies that the disturbance between two states ρ_1, ρ_2 has a lower bound, quantified by the gain in information due to measurements. The difference between disturbance, D_i ($\times 100\%$) and gain in information ($1 - H(\nu(p, t))$) ($\times 100\%$) as a function of t and precision p are shown in Figure 6a,b. We note that for the input parameters ($c_1 = c_2 = c=0.4, c_3=0.1$), there exists a range of p and t for which “information-disturbance relationship” is violated.

Comparing the results in Figure 6 a,b with those in Figures 2, 3, one notes that the appearance of increased quantum discord is invariably linked to the non-violation of the inequality in Eq. (28) when $c_3 > c$. The difference between the disturbance, D_i (Eq. (26)) and the mutual information ($1-H(\nu(p, t))$) yields a measure of the quantum discord. This difference is accentuated at increasing p , a trend that is also observed in the enhancement of the quantum discord \mathcal{D} at higher p . One can expect a zero discord when the lower bound in Eq. (28) is reach, at which point the disturbance on the system equates the amount of information that can be retrieved. Another important observation relates to the case when $c > c_3$, where we earlier noted the existence of a small $\mathcal{C} \approx 0.01$ and \mathcal{D} that was immune to changes in p . Interestingly, we note that a violation of Eq. (28) occurs when $c > c_3$ and for a range of p, t as illustrated in Figure 6b. This violation may be due to presence of other unknown subsystems present nearby, that result in a net deficit in quantum discord as far as the two known subsystems A, B are concerned. This results in greater retrieval of information than the actual disturbance on the system.

The results in Figure 6 a,b can partly be interpreted on the basis of earlier obtained results in Figure 1 a,b,c, where we noted that at higher $c > c_3$, there is trend towards violation of the CHSH-Bell inequality. The violation of Heisenberg’s “measurement-disturbance relationship” as evidenced by the nature of the c, c_3 input parameters, may have its origins in non-local quantum states which are also influenced by these same parameters. To this end, investigations involving more rigorous mathematical formulations [50] of the underlying abstract Hilbert space are needed to provide greater insight to the links between the information-disturbance tradeoff relation, quantum discord and quantum non-locality based on the CHSH-Bell inequality function \mathcal{B} (Eq. (16)). The results obtained here may be useful in the interpretation of experimental results [31] showing similar violation of the “measurement-disturbance relationship”.

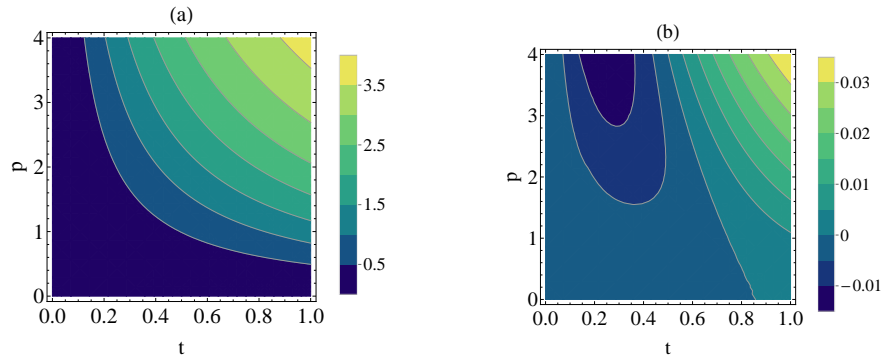


FIG. 6: (a) Contour-plots showing the trade-off between the measurement disturbance and information gain. Difference between disturbance, D_i ($\times 100\%$) and gain in information ($1-H(\nu(p, t))$) ($\times 100\%$) as a function of t and precision p . $\rho_1 = \rho_B^\parallel(t=0, p=0)$ and $\rho_2 = \rho_B^\parallel(t, p)$ (Eq. (20)). $c_1 = c_2 = c=0.1, c_3=0.7, g = \gamma\tau=0.5$ and $\theta=90$. (b) Description and parameters are the same as in (a) with the exception of $c_1 = c_2 = c=0.4, c_3=0.1$. A range of p and t for which the difference between disturbance, and gain in information is negative becomes noticeable.

VI. NON-MARKOVIANITY DURING QUANTUM MEASUREMENTS

To better understand the flow of information during quantum measurements, we consider the appearance of non-Markovianity, in relation to the attributes, p, t . Quantum systems undergoing Markovian dynamics observe a com-

pletely positive, trace preserving dynamical map $\Lambda(t)$, $\rho(0) \rightarrow \rho(t) = \Lambda(t)\rho(0)$, which constitutes the one parameter semi-group obeying the composition law [51–53], $\Lambda(t_1)\Lambda(t_2) = \Lambda(t_1+t_2)$, $t_1, t_2 \geq 0$. Accordingly, the fidelity function $F[\rho(t), \rho(t+\tau)]$ involving the initial state $\rho(t)$ and the evolved state $\rho(t+\tau)$ at a later time $t+\tau$, under Markovian dynamics satisfies the inequality [52]

$$\begin{aligned} F[\rho(t), \rho(t+\tau)] &\equiv F[\Lambda(t)\rho(0), \Lambda(t)\rho(\tau)] \\ &\Rightarrow F[\rho(t), \rho(t+\tau)] \geq F[\rho(0), \rho(\tau)]. \end{aligned} \quad (29)$$

Any violation of this inequality is a signature of non-Markovian dynamics which can be observed via the fidelity difference function

$$\Delta(t, \tau) = \frac{F[\rho(t), \rho(t+\tau)] - F[\rho(0), \rho(\tau)]}{F[\rho(0), \rho(\tau)]}, \quad (30)$$

Negative values of $\Delta(t, \tau)$ serve as sufficient but not necessary condition of non-Markovianity. Using Eq. (30), we have evaluated the fidelity difference $G(t, \tau)$ as a function of t and θ for the density matrices corresponding to $\rho_1 = \rho_B^\parallel(t=0, p=0)$ and $\rho_2 = \rho_B^\parallel(t, p)$ (Eq. (20)), as illustrated in Figures 7 and 8. The figures highlight important differences between systems where $c_3 > c$ and those with $c > c_3$. In regions midway with $25 < \theta < 42$, there is enhancement of non-Markovianity with precision p when $c_3 > c$. In systems where $c_3 < c$, the non-Markovian regions are located at the peripheral regions, $\theta \approx 0, 90$. We note that at $c_3 > c$ the optimized angle θ used in the evaluation of the classical correlation in Eq. (23) is about 90, decreasing gradually with increase p . At $c_3 < c$, the optimized angle $\theta < 30$. These results highlight the role of c, c_3 parameters on the links between non-Markovian dynamics and optimization processes associated with the classical correlation measure. These findings have implications in the violation of the “measurement-disturbance relationship” in Eq. (28). For instance, a possible pathway for violation of this relationship may be attained when gain in information exceeds disturbance between two states via non-Markovian processes. This possibility however require further investigation involving more generalized systems, as numerical results related to just two subsystems have been provided here.

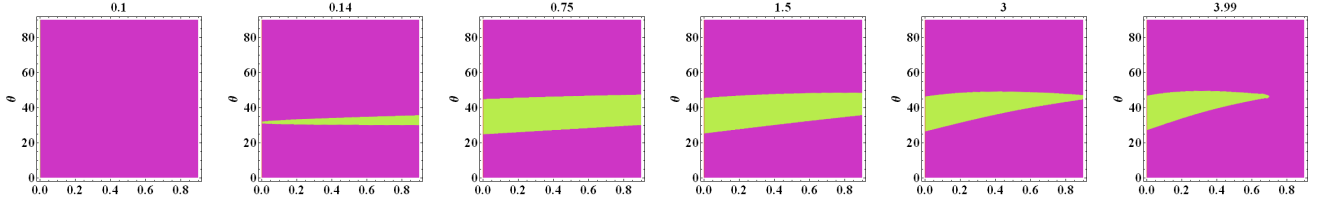


FIG. 7: Fidelity difference $\Delta(t, \tau)$ as a function of t and θ for the density matrices corresponding to $\rho_1 = \rho_B^\parallel(t=0, p=0)$ and $\rho_2 = \rho_B^\parallel(t, p)$ (Eq. (20)). We set $\tau=0.1$, $c_1 = c_2 = c=0.1$, $c_3=0.8$, $g = \gamma\tau=0.1$. Values of p are indicated at the top of each figure. Negative values indicating non-Markovianity are shaded green, increases with precision p and are dominant around $25 < \theta < 42$.

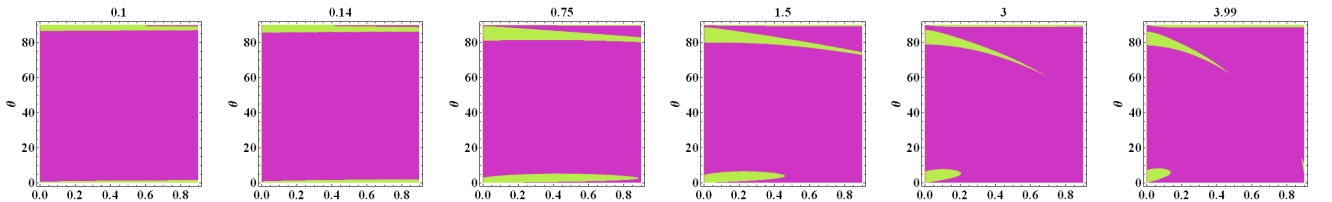


FIG. 8: Fidelity difference $\Delta(t, \tau)$ as a function of t and θ for the density matrices corresponding to $\rho_1 = \rho_B^\parallel(t=0, p=0)$ and $\rho_2 = \rho_B^\parallel(t, p)$ (Eq. (20)). We set $\tau=0.1$, $c_1 = c_2 = c=0.4$, $c_3=0.1$, $g = \gamma\tau=0.1$. Values of p are indicated at the top of each figure. Negative values indicating non-Markovianity are shaded green and are located at the peripheral regions, $\theta \approx 0, 90$.

VII. CONCLUSION

In conclusion, we have presented results of the influence of non-ideal attributes such as the measurement precision and finite measurement time duration on the classical correlation and quantum discord for a qubit pair immersed in a common environment. The results obtained show that the quantum discord is enhanced as the precision of

the measuring instrument is increased for a range of parameters, and both the classical correlation and the quantum discord undergo noticeable changes during the duration when measurements are performed on a neighboring partition. We also conclude that increased quantum discord within two subsystems, is invariably linked to the non-violation of the inequality associated with the “information-disturbance relationship”. We note that a zero discord corresponds to the lower bound in this inequality, consistent with the point at which the disturbance on the system equates the amount of information that can be retrieved. A violation of this inequality indicates a deficit in quantum discord, possibly due to presence of other unknown subsystems, giving rise to a greater retrieval of information than the actual disturbance on the system. This shows that the fundamental limits of quantum mechanical measurements can be influenced by non-classical correlations such as the quantum discord.

The violation of the “information-disturbance relationship” may have links with quantum non-locality and non-Markovian quantum dynamics of states that do not necessarily evolve via a completely positive, trace preserving dynamical maps. This studies identifies (although not conclusively) that a possible pathway for violation of this relationship may occur when gain in information exceeds disturbance between two states via non-Markovian processes. Further scrutiny of the intricate links between these entities require mathematically rigorous approaches [50] and experimental verifications, however the results here have wider implications for exploiting the subtleties of the Uncertainty Principle. Cryptographic technologies specify that eavesdroppers can be detected as a result of disturbances caused by their measuring activities. The results obtained here indicates that eavesdroppers can remain undetected in some instances (when positivity of the density matrix of the observed system is violated). Lastly, this study shows that the joint examination of several entities (non-locality, non-Markovianity, negative quantum discord) is needed in investigations involving quantum measurements of optics and nanostructure systems [54, 55]. The possibility that an analogous “information-disturbance relationship” may be violated in light-harvesting systems [56–60] is an area for future investigation of systems which display exceptionally high efficiencies of energy transfer processes.

VIII. ACKNOWLEDGEMENTS

This research was undertaken on the NCI National Facility in Canberra, Australia, which is supported by the Australian Commonwealth Government. The author gratefully acknowledges the support of the Julian Schwinger Foundation Grant, JSF-12-06-0000. The author would like to thank R. Jansi and I. K. Oh for useful discussions.

References

-
- [1] J. von Neumann, “Mathematical Foundations of Quantum Mechanics,” Princeton University Press, Princeton, (1955).
 - [2] H.D.Zeh, *Found. Phys.* **1**, 69 (1970).
 - [3] A. G. Kofman, G. Kurizki, *Nature* **405**, 546 (2000); *Phys. Rev.A* **54**, 3750(R)(1996).
 - [4] B. Misra and E. C. G. Sudarchan, *J. Math. Phys.* **18**, 758 (1977).
 - [5] P. Busch, P. J. Lahti, and P. Mittelstaedt, “The Quantum Theory of Measurement,” Springer-Verlag, Berlin, (1991).
 - [6] W.M. Itano, D. J. Heinzen, J. J. Bollinger and D. J. Wineland, *Phys. Rev.A* **41**, 2295 (1990).
 - [7] P. Facchi and S. Pascazio, *J. Phys. A: Math. Theor.* **41** 493001 (2008); P. Facchi and S. Pascazio, *Phys. Rev. Lett.* **89**, 080401 (2002).
 - [8] V. B. Braginsky and F. Ya. Khalili, “Quantum Measurement”, K. S. Thorne editor (Cambridge University Press, Cambridge) (1992), and references cited therein.
 - [9] M. B. Mensky, “Continuous Quantum Measurements and Path-Integrals” (Institute of Physics Publishers, Bristol and Philadelphia) (1993).
 - [10] W. H. Zurek, *Phys. Today* **44** (10), 36 (1991).
 - [11] W. H. Zurek, *Phys. Rev. D* **26**, 1862 (1982).
 - [12] M. Schlosshauer, “Decoherence and the Quantum-to-Classical Transition”, Springer-Verlag, (2008).
 - [13] R. Ruskov and A. N. Korotkov, *Phys. Rev. B* **67**, 241305(R) (2003).
 - [14] J. Kofler and C. Brukner, *Phys. Rev. Lett.* **99**, 180403 (2007).
 - [15] J. Kofler and C. Brukner, *Phys. Rev. Lett.* **101**, 090403 (2008).
 - [16] H. Ollivier and W. H. Zurek, *Phys. Rev. Lett.* **88**, 017901 (2001).
 - [17] L. Henderson and V. Vedral, *J. Phys. A* **34**, 6899 (2001).
 - [18] V. Vedral, *Phys. Rev. Lett.* **90**, 050401 (2003).
 - [19] V. Coffman, J. Kundu and W. K. Wootters, *Phys. Rev. A* **61**, 052306 (2000).
 - [20] A. Brodutch and D.R. Terno, *Phys. Rev. A* **81**, 062103 (2010).

- [21] J. Maziero, L. C. Céleri, R. M. Serra and V. Vedral, Phys.Rev. A **80**, 044102 (2009).
- [22] L. Mazzola, J. Piilo and S. Maniscalco, Phys. Rev. Lett. **104**, 200401 (2010).
- [23] L. Ciliberti, R. Rossignoli and N. Canosa, Phys. Rev. A **82**, 042316 (2010).
- [24] A. Datta, A. Shaji, and C. M. Caves, Phys. Rev. Lett. **100**, 050502 (2008).
- [25] M. F. Sacchi, Phys. Rev. Lett. **96**, 220502 (2006).
- [26] L. Maccone, Phys. Rev. A **73**, 042307 (2006).
- [27] G. M. Ariano, Fortschr. Phys., **51**, 318 (2003).
- [28] F. Buscemi and M. F. Sacchi, Phys. Rev. A **74**, 052320 (2006).
- [29] L. Maccone, EPL **77**, 042307 (2006).
- [30] W. Heisenberg, *The physical principles of the Quantum Theory*, Dover (1930).
- [31] L. A. Rozema, A. Darabi, D. H. Mahler, A. Hayat, Y. Soudagar, and A. M. Steinberg, Phys. Rev. Lett. **109**, 100404 (2012)
- [32] R. P. Feynman and A. R. Hibbs, *Quantum Mechanics and Path Integrals*, (McGraw-Hill, New York) (1965).
- [33] R. P. Feynman, Rev. Mod. Phys. **20**, 367 (1948).
- [34] M. B. Mensky, Phys. Rev. D **20**, 384 (1979); Sov. Phys. JETP **50**, 667 (1979).
- [35] M. B. Mensky, R. Onofrio, and C. Presilla, Phys. Rev. Lett. **70**, 2825 (1993).
- [36] M. B. Mensky, R. Onofrio, and C. Presilla, Phys. Lett. A **161**, 236 (1991).
- [37] R. Onofrio, C. Presilla, and U. Tambini, Phys. Lett. A **183**, 135 (1993).
- [38] U. Tambini, C. Presilla, and R. Onofrio, Phys. Rev. A **51**, 967 (1995).
- [39] J. Ausretsch and M. Mensky, Phys. Rev. A **56**, 44 (1997).
- [40] A. Thilagam, J. Phys. A **45**, 444031 (2012).
- [41] W. D. Heiss, Phys. Rev. E **61**, 929 (2000).
- [42] A. Salles, F. de Melo, M. P. Almeida, M. Hor-Meyll, S. P. Walborn, P. H. Souto Ribeiro, and L. Davidovich, Phys. Rev. A **78**, 022322 (2008).
- [43] E.C.G. Sudarshan, P.M. Mathews, J. Rau, *Stochastic Dynamics of Quantum-Mechanical Systems*, Phys. Rev. Vol.121 No.3, 920-924 (1961)
- [44] K. Kraus, "States, Effects, and Operations: Fundamental Notions of Quantum Theory", Springer (1983).
- [45] J.S. Bell, Physics **1**, 195 (1964).
- [46] J.F. Clauser, M.A. Horne, A. Shimony, R.A. Holt, Phys. Rev. Lett. **23**, 880 (1969).
- [47] B. Bellomo, R. LoFranco and G. Compagno, Phys. Rev. A **78**, 062309 (2008).
- [48] F. Galve, G. L. Georgi and R. Zambrini, "Orthogonal measurements are almost sufficient for quantum discord of two qubits", arXiv:1107.2005 v2 (2011).
- [49] R. Jozsa, J. Mod. Opt. **41**, 2315 (1994)
- [50] J. Anandan and Y. Aharonov, Phys. Rev. Lett. **65**, 1697 (1990).
- [51] M.M. Wolf, J. Eisert, T.S. Cubitt, and J.I. Cirac, Phys. Rev. Lett. **101**, 150402 (2008).
- [52] A. K. Rajagopal, A. K. UshaDevi, R. W. Rendell, Phys. Rev. A **82**, 042107 (2010).
- [53] H.-P. Breuer, E.-M. Laine, J. Piilo, Phys. Rev. Lett. **103**, 210401 (2009)
- [54] M. A. Hall, J. B. Altepeter and P. Kumar, Optics Express **17**, 14558 (2009).
- [55] W. Tittel, J. Brendel, H. Zbinden, and N. Gisin, Phys. Rev. Lett. **81**, 3563 (1998).
- [56] F. Caruso, A. W. Chin, A. Datta, S. F. Huelga, and M. B. Plenio, J. Chem. Phys. **131**, 105106 (2009).
- [57] P. Rebentrost, M. Mohseni, and A. Aspuru-Guzik, J. Phys. Chem. B **113**, 9942 (2009).
- [58] A. Thilagam, J. Chem. Phys. **136**, 065104 (2012), J. Chem. Phys. **136**, 175104 (2012).
- [59] A. Thilagam and A. R. U. Devi, J. Chem. Phys. **137**, 215103 (2012).
- [60] J. R. Caram, A. F. Fidler, and G. S. Engel, J. Chem. Phys. **137**, 024507 (2012).